GDMS Analysis of Calcium Carbonate Naturaly Doped by REE, Phospates and other Impurities

V.D. Kurochkin*, O.M. Romanenko

Frantsevich Institute for Problems of Materials Science NAS of Ukraine, 3, Krzhyzhanovsky str., Kyiv-142, 03680, Ukraine; *e-mail: vkur46@gmail.com

Recieved: April 24, 2019; Accepted: August 16, 2019
DOI: 10.17721/moca.2019.91-101

A mathematical model was developed for calculation of types and intensities of molecular interferences and simulation of mass-spectra at GDMS analysis of non-conducting samples with the use of a secondary cathode. An improved design of the cell with Ta-secondary cathode were suggested enhancing the matrix to tantalum ion current ratio and sensitivity of the analysis in ca. 1.5 orders of magnitude. The model have been used for interpretation of complicate mass-spectra of calcium carbonate naturally doped with REE, phosphates and other impurities. Comparison calculated and experimental mass-spectra of VG9000 instrument demonstrates good agreement and allows select the most suitable isotopes and rejecting wrong molecular peaks. It have been shown that electrons in glow discharge plasma have different temperatures in different zones that reveals itself as separate Boltzmann populations of ionization levels for molecules, metal atoms and argon atoms/ions. Calcium carbonate is widely used for many application including as precursor for nano-hydroxyapatite synthesis. Calcium carbonate was precipitated from natural mine waters and was used as model object having high number of various impurities allowing to investigate the impact of complicate molecular ions, determine necessary resolving power of the GD-instruments to meet required detection limit.

Keywords: glow discharge mass-spectrometry, calcium carbonate, rare earth elements, hydroxyapatite doped with REE, mathematical simulation of mass spectra

Аналіз карбонату кальцію природно легованому РЗЕ, фосфатами та іншими домішками методом мас-спектрометрії із жевріючим розрядом

В.Д. Курочкін*, О.М. Романенко

Інститут проблем матеріалознавства ім. І.М. Францевича НАН України, вул. Кржижановського 3, м. Київ, 03680, Україна; *e-mail: vkur46@gmail.com

Надійшла: 24 квітня 2019 р; Прийнята: 16 серпня 2019 р
DOI: 10.17721/moca.2019.91-101

Розроблено математичну модель для розрахунку типів та інтенсивності молекулярних перешкод та моделювання мас-спектрів при мас-спектрометричному аналізі із жевріючим розрядом непровідних зразків з використанням вторинного катода. Запропоновано поліпшену конструкцію комірки з Та-вторинним катодом, що підвищує відношення струму іонів матриці до танталу і чутливість аналізу приблизно на 1.5 порядки. Модель використовувалася для інтерпретації складних мас-спектрів карбонату кальцію, природно легованого РЗЕ, фосфатами та іншими домішками. Порівняння розрахованих і експериментальних мас-спектрів приладу VG9000 демонструє хорошу згоду і дозволяє обирати найбільш підходящі ізотопи та відкидати помилкові молекулярні піки. Показано, що електрони в плазмі тліючого розряду мають різні температурами в різних зонах, що виявляється як окремі Больцманівські заселеності рівнів іонізації для молекул, атомів металів і атомів та іонів аргону. Карбонат кальцію широко використовується для багатьох застосувань, зокрема як вихідний реагент для синтезу нано-гідроксиапатиту. Карбонат кальцію осаджувався з природних шахтних вод і використовувався як модельний об'єкт, що має велику кількість різних домішок, що дозволяє досліджувати вплив складних молекулярних іонів, визначати необхідну роздільну здатність GD-приладів для досягнення необхідної межі визначення.

Ключові слова: мас-спектрометрія жевріючого розряду, рідкоземельні елементи, гідроксіапатит легований РЗЕ, математичне моделювання мас-спектру

Glow discharge mass-spectrometry (GDMS) method is recognized as one of the most sensitive and universal method for analysis of all elements and isotopes of periodical system with sensitivity at ppb and even at ppt level. High resolution GDMS-spectrometers such as VG9000 allows simultaneous analysis in a single scan both major constituents and trace elements. One of the advantages of the method is weak dependence of relative sensitivity factors (RSFs) from the matrix, that allows semi-quantitative analysis of samples without calibration by means of standard reference materials.

A common problem of mass spectrometric methods, regardless of the method of ions formation, are isobaric interferences caused by the presence in the plasma of isotopes of other elements with the same nominal mass, doubly charged ions, polyatomic clusters, which may not be resolved enough from the isotopes under study [1, 2]. Their effect is significant even on doubly-focusing spectrometers such as VG9000 at a high resolution at half a peak height ($R_{0.5}$ = m / Δm) of about 7000 - 9000. For quadrupole mass spectrometers with lower resolution, this problem is even more acute. The solution to the problem was proposed earlier and consists in calculating the concentration and types of possible molecular ions in the mass range of the isotopes under study [3]. In the present paper are discussed molecular interferences arising at analysis of calcium carbonate naturally doped with REEs, which was obtained as a precipitate from mine waters of Donetsk region. This type of samples is interesting both from geological point of view and as model object serving as precursor for hydroxyapatite (HAP) synthesis. Calculations were performed with the new version of the computer program allowing more precise calculation polyatomic ions on the basis of refined effective equilibrium constants measured for the matrix discussed.

Hydroxyapatite is widely used as material for modern biological and other applications so elaboration of new analytical methods for high sensitivity analysis may promote the progress in these fields. HAP is used as material for bone implants, thanks to its excellent biological compatibility, biodegradability, and bioactivity. Rare earth doped apatite nanoparticles have the ability to emit near infrared radiations and is suitable for biological system imaging as fluorescence labeling agent. These particles can emit various colors depending on the type of lanthanide dopant ions such as Ce^{3+}, Pr^{3+}, Nd^{3+}, Sm^{3+}, Eu^{3+}, Tb^{3+}, Dy^{3+}, Er^{3+}, Tm^{3+}, and Yb^{3+}. The near infrared emission is of low absorptivity by tissue chromophores and especially suitable for biological system [4]. HAP was also successfully used as an alternative low-cost adsorbent material to study the adsorption behavior of La^{3+} and Eu^{3+} ions from nitrate aqueous solutions [5]. Nano-hydroxyapatite functionalized by arginine and doped with rare earth elements such as Tb^{3+}, is suitable for the application of gene delivery as a gene carrier [6]. Eu-doped HAP-nanoparticles demonstrates the antimicrobial activity that extends the area of its application and required reliable methods of its characterization [7]. One of the most popular synthesis techniques for producing hydroxyapatite powders is a hydrothermal technique that involves reaction of calcium carbonate ($CaCO_3$) with di-ammonium hydrogen phosphate at high temperatures and pressures. Taking into account above applications of HAP it is clear that developing of reliable methods of analysis of samples based on calcium carbonate matrix doped with REE elements, phosphates, sulfates and other impurities is actual task.

Sample preparation and instrumentations

Glow discharge mass-spectrometry uses cathode sputtering by Ar ions that suppose the sample material to be conducting. In the analysis of non-conducting materials, the technique of secondary cathode is used or mixing the powder sample with conducting binder [8 – 15]. Material of secondary cathode and its assembly significantly influences on results of analysis. It must meet several important requirements to successfully carry out its functions. First of all, it must ensure necessary conductance of a sample, stable discharge conditions and sputtering rate. Matrix current must be sufficiently high and have comparable value with the secondary cathode current to ensure required sensitivity of the analysis.

Second trivial, but not always available property is the purity of the cathode for elements to be analyzed. In the present study we have explored Ta of high purity (5N). Another important property of the cathode metal is its ability not creating molecular interferences in the mass range of detected isotopes. For this purpose it is desirable to use metals with an odd charge of the nuclei, which are monoisotopic or has two isotopes, one of which, as a rule, has a low abundance and appropriate mass.

Analysis of solid samples with secondary cathode by known techniques is conducting mainly by means of metal foil with orifice ca. 4 – 5 mm. During presputtering time the steady state is established. Continuous, in situ sputter-redeposition from the secondary cathode metal (Cu, Ag, Ta) results in thin conducting layer on the surface of a sample making it conducting. The thickness of the metal film is of great importance, because it must allow argon ions penetrate the film and sputter covered sample. Reported relation $^{30}Si/^{180}Ta$ at analysis of glass with secondary cathode as a foil with orifice, however, is ca. 4, that is in recalculation to the 100 % abundances matrix current in 2 order of magnitude smaller than Ta-current (0.01) [9]. Advantage of such cathode design is simple procedure of sample preparation in the case of a sample available with clean flat surface. If it is necessary to polish raw polycrystalline surface it became a problem with its contamination and subsequent cleaning. Nevertheless, the ratio of matrix

to secondary cathode current remains rather low (0.01) and restricts sensitivity of an analysis. Another difficulty of this technique is poor stability of the matrix current because of changing of the diameter of the orifice owing to sputtering in process of time.

It is also known techniques of the secondary cathode using a mesh, foil, artificial wool of silver or indium of high purity. For this method, the samples were transferred to a solution, precipitated on a grid and dried [16]. The disadvantage of this method is the need to transfer the tested sample into a solution.

In the present paper we have used secondary cathode as a tantalum flat slab of 2 – 3 mm of thickness. Powder sample was deposited as a thin layer, rubbed in tantalum with high purity sapphire rod. Design of the flat cell is shown in the Fig. 1.

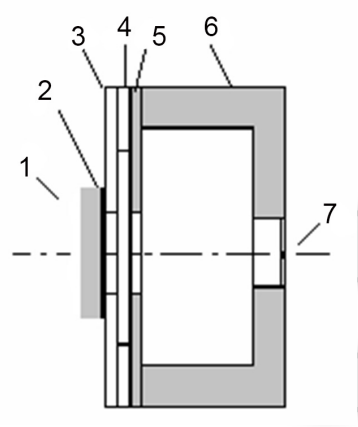

Fig. 1. 1 – Ta cathode plate, 2 – nonconducting sample, 3, 4 – sapphire spacers, 5 – anode plate, 6 – cell, 7 – outlet orifice.

Two insulating spacers from high purity sapphire one with diameter 8 – 10 mm and second with diameter 20 mm provide good insulation because greater diameter of the ring 4 prevents it from tantalum deposit and from short circuit. Glow discharge parameters of VG9000 instrument [3] was as follows: voltage: 700 – 800 V, current – 2 mA. This method excludes pressing of pellets, requires very small amount of a sample (ca. < 5 mg) and, that is especially important, provides high ratio of matrix current to Ta current ($I(^{44}Ca)/I(^{181}Ta)$ = 0.0046). Taking into account abundances of isotopes ^{44}Ca and ^{181}Ta and calcium content this relation is much more better (ca. 0.5) than in the case of Ta-cathode foil with orifice applied on the surface of the sample (Imatrix / I(Ta) = 0.01) (Fig.2). As the concentration is calculated by normalization of isotope current by the matrix current this means enhancing of sensitivity up to 2 orders of magnitude.

The same design of the secondary cathode has been utilized also for analysis of high purity sapphire [17]. Ta-slab after analysis may be easily cleaned by HF + HNO_3 acid. Tantalum is etched by the acid thus poorly soluble particles of a sample freely removed from the surface of the cathode.

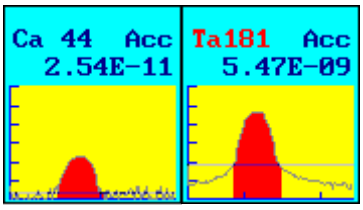

Fig. 2. Integral ion currents of the matrix (Ca) and Ta secondary cathode.

At analysis of complex nonconducting systems such as geological objects, carbonates, oxides etc. special attention must be paid for proper calibration, taking into account influence of the secondary cathode material on the oxygen, carbon and hydrogen concentration. Gaseous components significantly contribute into matrix current in such cases so standard reference materials must have as close composition to the samples as possible.

Method of molecular interferences calculation. The main principles of calculation of molecular ions concentration in Ar-glow discharge plasma have been reported for the first time in the paper devoted to the GDMS analysis aluminum alloys [3] and have found further development for non-conducting samples [17, 18]. The method based on the use of effective equilibrium constants (EEC) of the ion-molecular reactions.

In the previous study have been shown, that formation of ionic dimers goes through the intermediate excited quasi-stable complex that goes into the molecular ion by monomolecular reaction with radiation (Lindeman reaction scheme). That manifested itself as quasi-monomolecular reaction despite two reagents interacting to form ionic dimers [19, 20]. As a result at constant voltage increasing in current and argon pressure concentration of molecular ions of ArX^{+1} type has a maximum. Enhanced pressure is responsible for this effect because it accelerates not only deactivation of intermediate complex but also collisional dissociation of molecular ions. Increasing in current and voltage at constant pressure results in linear increasing of argon dimers concentration. That is why enhanced pressure is needed to minimize contribution of molecular ions. Cooling of the cell by liquid nitrogen in the case of carbonates analysis can not decrease molecular ion concentration. Moreover, collsionally-induced dissociation of molecular ions in the cryo-cooled cell is less active that results in enhanced molecular ion concentration in 1 – 1.5 order of magnitude compared to the “hot” cell.

Reactions of sample components with material of secondary cathode strongly affected the plasma composition. Tantalum has high affinity to the oxygen and substantially influenced on the equilibrium composition of molecular ions and therefore on the EECs. Tantalum may be easily cleaned in “aqua regia” and is applicable for most elements of periodical

system that are lighter than tantalum. However, it creates strong interferences with gases that affected determination of Au and Pt ($^{181}Ta^{16}O$ – ^{197}Au, $^{181}Ta^{13}C$ – ^{194}Pt, $^{181}Ta^{14}N$ – ^{195}Pt and others). The specific interferences in this region of masses and other interferences in more details will be discussed in the next section.

Results and discussion

Effective equilibrium constants were determined experimentally using known values of components concentration. Measurements were performed in suitable mass range where concentration of other molecular ions was as low as possible. Experiments show that EECs for molecular ions of MeO^{+1} type correlate with energy of dissociation of molecules of corresponding oxides and are in the range 10^{-7} – 10^{-6} ppm^{-1}.

Despite glow discharge plasma is non-equilibrium object, temperature of heavy particles is of about ambient conditions but electrons may have Maxwell distribution function with defined temperature in certain plasma areas. This effect may be demonstrated using dependence of ion current for metals and argon ions (Fig. 3). Temperature calculated from distribution of ions Ar^{+1} – Ar^{+3} comprises kT ~ 4.5 eB (T ~ 50 000 K). But ions Ar^{+6} – Ar^{+4} are formed in hotter region of plasma with temperature kT ~ 7 eB, which is in good agreement with results of work [21]. Temperature, calculated for ions Cr^{+1}, Cr^{+2}, Cr^{+3} is of about 1.5 eV. Analogous calculation for the molecular ions MeO^{+1} gives temperature ~ 0.75 eV. These rules allow refine EECs and show that ions of argon, metals and molecular ions are formed in different areas of the GD plasma.

In the previous work we have studied molecular interferences at analysis of dry sediments of mine water with sodium sulfate and iron oxide matrix and high Ba-content [18]. The main interferences in the region of REEs were produced by barium sulfides, sulfates, oxides and hydrides. This region of masses is of interest since REE are natural dopant for $CaCO_3$ precipitated from some types mine waters of Donetsk region. Complete composition of the dry sediments of the sample #1 (KO-IV39) is presented in the table 1. For these concentrations were calculated molecular interferences. Concentrations of gases and gas forming elements are results of equilibrium processes of accumulation from the sample and redistribution over various nonvolatile molecules (tantalum oxides, carbides, nitrides, calcium oxides and others). So they represent not the true concentration in the sample, but concentration in the cell, calculated by dividing ion currents of these elements by the matrix current and were used for calculation of molecular interferences.

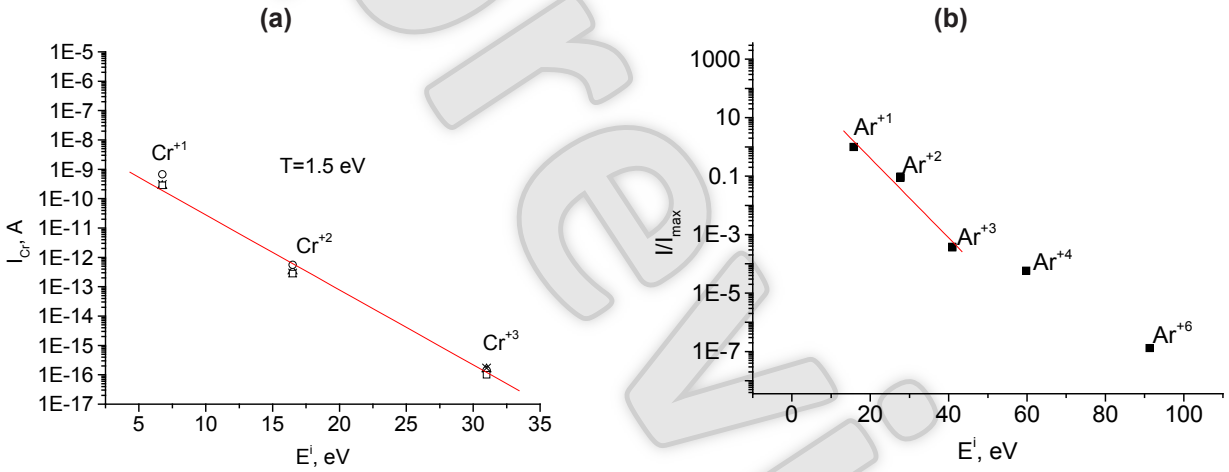

Fig. 3. Currents of Cr and Ar ions as function of ionization potential.

Table 1. Composition of the sample #1(KO-IV39) which was used as model object of $CaCO_3$ matrix for molecular ions study.

Element	Concentration, ppm	Element	Concentration, ppm
$H^{(1)}$	5.00E+04	Mo	2.00E+01
$C^{(1)}$	2.10E+05	Ba	9.00E+01
$N^{(1)}$	8.00E+04	La	1.80E+02
$O^{(1)}$	9.00E+04	Ce	5.70E+02
F	2.00E+03	Pr	9.00E+01
Na	6.80E+03	$^{145}Nd^{(2)}$	4.30E+02
Al	9.20E+02	^{146}Nd	4.30E+02

Table 1. (continuation).

Element	Concentration, ppm	Element	Concentration, ppm
Si	8.00E+02	Sm	1.40E+02
P	3.40E+03	^{151}Eu	3.90E+01
S[(1)]	1.20E+04	^{153}Eu	4.00E+01
Cl	5.20E+02	^{155}Gd	4.40E+02
Ca	5.20E+05	^{157}Gd	2.80E+02
Sc	4.30E+02	Tb	3.00E+01
Mn	4.50E+02	Dy	1.30E+02
Fe	4.40E+03	Ho	2.30E+01
Ni	1.60E+02	Er	6.00E+01
Cu	3.80E+02	^{172}Yb	6.80E+01
Zn	5.30E+02	^{173}Yb	6.90E+01
Sr	1.00E+03	Ta[(3)]	(6.00E+06)
Y	4.80E+02	Pb	2.60E+03
Zr	2.20E+02	Bi	2.60E+02
Nb	3.00E+01	Th	1.60E+02
Cd	1.60E+02	U	2.00E+01

[(1)] – effective concentration, used for calculations of molecular interferences; [(2)] – Isotopes are given for estimation of molecular ions impact; [(3)] – Ion current of the Ta-secondary cathode was excluded from matrix current.

This type of waters is featured by high content of REE. The relative ratio of REE in more details is presented in the Fig. 4. Despite there are no elements between every point, i.e. diagram is discrete in definition, it is generally accepted to join points by the line to facilitate its visual perception.

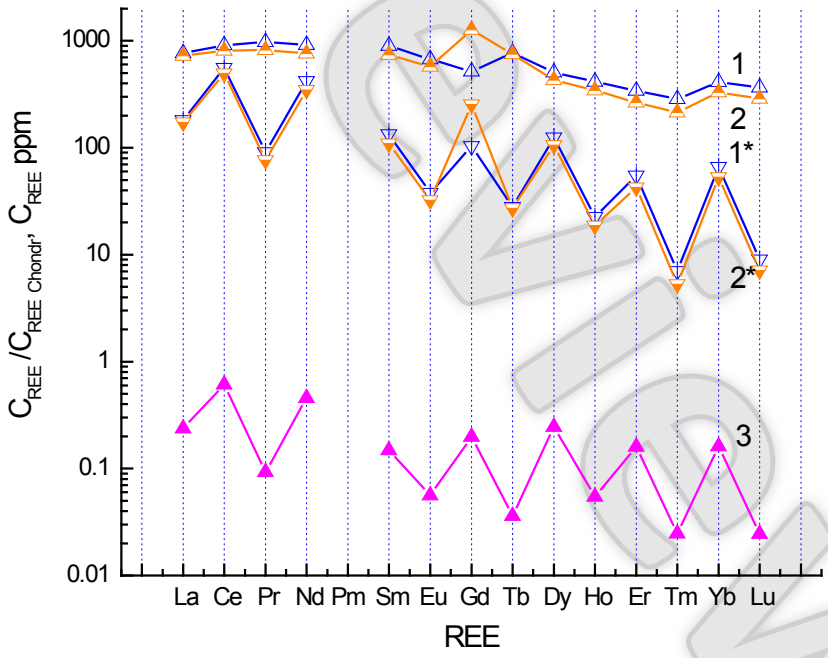

Fig. 4. 1, 2 – normalized values by the chondrite concentrations for samples #1 and #2 (relative units); 1*, 2*, 3 - concentrations (ppm) for samples #1 and #2 and chondrite respectively.

Along with concentration in the Fig. 4 are shown so called “spider diagrams”, i.e. concentration normalized by chondrite meteorites concentration. Relative ratio of REEs concentrations in hondrites is considered as unchanged archetypal since the time of the solar system formation and even earlier, as REEs are born during the outbreaks of the supernovas. Concentration plot is featured by known rules – REEs with odd nucleus charge are less abundant than elements with even nucleus charge and concentration of light REE (LREE) are greater than that of heavy REE (HREE). Experimental results obey these rules that is additional prove of their correctness. Spider diagram from La to Dy shows small deviation of relative abundance of these elements from chondrite concentration, despite absolute values in water sediments are in 3 orders of magnitude greater. Absolute values of REEs concentration for these samples in 1.5 order of magnitude greater than average content of these elements according to the data for so called “North American shale composite”, that represents average REEs content in the earth crust [22]. Results show substantial enrichment of some samples of mine water sediments by REEs. We will not discuss the geological reason of this effect because it is out of margins of the paper and restrict ourselves by the problems of GDMS analysis of such systems.

High content of calcium, carbon, oxygen, hydrogen and molecules of CO_2, CO, C_2, CH and others creates molecular interferences of types $ArMol^{+1}$, $IsMol^{+1}$ – combinations of gas molecules with argon isotopes and components of the sample, molecules of types $Is1_nIs2_m^{+1}$, $Is1_nIs2_mIs3_l^{+1}$ where Is1, Is2, Is3 – isotopes of sample components, gases and gas-forming elements (H, C, N, O, F, S, Cl). In the Fig. 5 and Table 2 are presented experimental mass spectra and calculations for elements important because of their biological activity (including toxic elements) and the most problematic because of molecular interferences.

The general rule for major 2 – 3 atomic interferences location for elements from ^{24}Mg to ^{90}Zr is the right side compared to the isotope measured, i.e. their m/q greater than that for the isotope. Gradually they group close to the centre of the line for isotopes in the mass range $^{95}Mo^+$ – ^{119}Sn. This mass range is mostly affected by interferences and requires close inspection of each isotope.

Special attention must be paid for monoisotopic elements, because there is no alternative isotope that would be used for the control of results obtained. Even precise mass-mark can’t ensure correctness of the result because of possible small temperature drift of the spectra. This is actual in analysis even resolved peaks, for instance ^{24}Mg. The system may tag also $^{48}Ca^{2+}$ or molecular ion $^{12}C_2^+$ as magnesium and simulated shape of mass-spectrum really can help make correct decision what is the true peak of $^{24}Mg^+$.

Measured current of ^{75}As is equivalent to 48 ppm concentration, but calculated intensity of sum interferences (Fig. 5, Table 2) are equal to 51 ppm that point out that measured peak must be rejected and concentration in the sample does not exceed 50 ppm. Similar calculations were made for about 100 isotopes of the periodic system, but in the paper we can present only small part of the data for the lack of space.

Certain difficulties arise in determining ^{52}Cr in a matrix that contains large concentrations of carbon and Ca due to the presence of molecular ions $^{40}Ar^{12}C^+$ and $^{40}Ca^{12}C^+$. Despite these peaks are well resolved at $R_{0.5} > 7000$ high background level should be taken into account. The same remarks are valid for ^{56}Fe ion with close peaks of $^{40}Ar^{16}O^+$ and $^{40}Ca^{16}O^+$.

Problems with Se determination by GDMS method in Ar-plasma due to the severe Ar_2 molecular ions are well established ($^{40}Ar^{36}Ar^+$ - ^{76}Se, $^{40}Ar^{38}Ar^+$ - ^{78}Se, $^{40}Ar_2^+$ - ^{80}Se) [23]. Isotope ^{82}Se in Ca-containing matrix is even less fit because of intense molecular peaks $^{40}Ar^{42}Ca^+$, $^{40}Ca^{42}Ca^+$ (~ 400 ppm) that are not sufficiently resolved even at resolution power $R_{0.5} > 20000$.

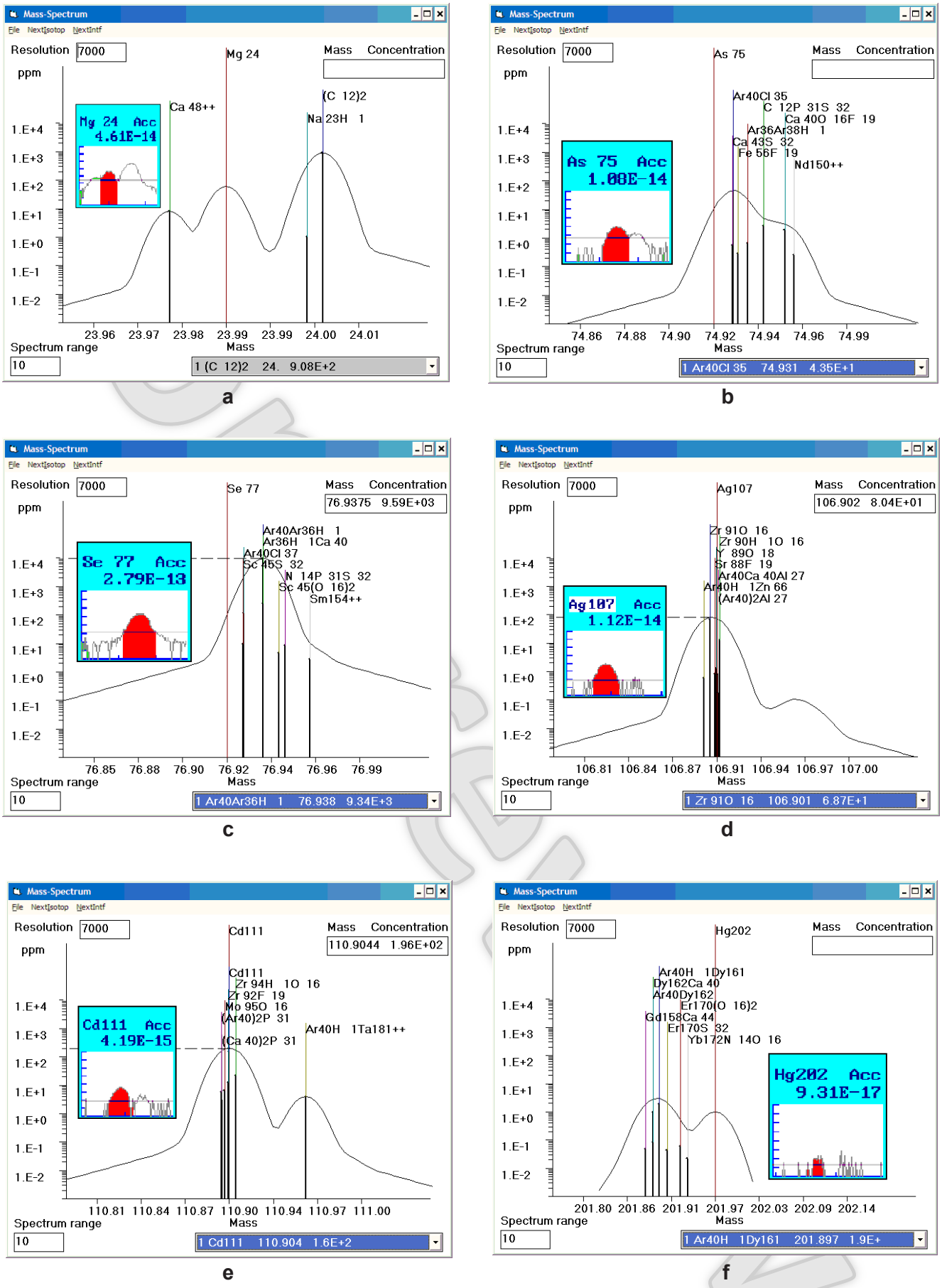

Fig. 5. Measured and calculated mass-spectra for some biologically active and toxic elements.

Table 2. Molecular interferences and detection limit for some elements (biologically active, toxic) in $CaCO_3$ matrix with impurities.

Isotope, molecular ion	Mass (m/q)	Maximal «concentration», ppm	Detection limit in dry sediment at $R_{0.5}$= 9000, ppm*
1	2	3	5
^{9}Be	**9.012182**		
O^{+2}	8.9996	<1	> 1
^{52}Cr	**51.94051**		> 1
$^{40}Ar^{12}C^{+}$	51.96238	8250	
$^{40}Ca^{12}C^{+}$	51.96259	1160 background	
^{56}Fe	**55.93494**		> 5
$^{40}Ca^{16}O^{+}$	55.95750	9650	
$^{40}Ar^{16}O^{+}$	55.95730	8800	
$^{44}Ca^{12}C^{+}$	55.95549	20	
^{75}As	**74.92159**		> 10
$^{40}Ar^{35}Cl^{+}$	74.93124	43	>1 without Cl
$^{12}C^{31}P^{32}S^{+}$	74.94583	3	
$^{40}Ca^{16}O^{19}F^{+}$	74.95590	2	
$^{36}Ar^{38}Ar^{1}H^{+}$	74.93810	0.7	
$^{43}Ca^{32}S^{+}$	74.93085	0.6	
$^{40}Ca^{35}Cl^{+}$	74.93144	0.2	
^{77}Se*	**76.91991**		> 150
$^{40}Ar^{36}Ar^{1}H^{+}$	76.93776	9300	
$^{40}Ca^{36}Ar^{1}H^{+}$	76.93796	260	
$^{40}Ar^{37}Cl^{+}$	76.92828	120	
$^{45}Sc^{32}S^{+}$	76.92799	10	
^{79}Br	**78.91833**		> 2
$^{40}Ar^{38}Ar^{1}H^{+}$	78.93294	86	
$^{40}Ca^{38}Ar^{1}H^{+}$	78.93314	3	
^{85}Rb	**84.91180**		> 10
$^{44}Ca^{40}Ar^{1}H^{+}$	84.92570	55	>1 without Sc
$^{40}Ar^{45}Sc^{+}$	84.91830	10	
$^{40}Ca^{45}Sc^{+}$	84.91850	0.4	
^{87}Rb	**86.90919**		>0.1 without Sr
$^{87}Sr^{+}$	86.90889	(380)	
$^{40}Ca^{16}O^{31}P^{+}$	86.93127	3	
^{88}Sr	**87.90562**		> 1
$^{40}Ar^{48}Ca^{+}$	87.91492	3	
$^{40}Ca^{48}Ca^{+}$	87.91512	1	
$^{56}Fe^{32}S^{+}$	87.90701	0.2	
^{95}Mo	**94.90584**		> 10
$^{40}Ar^{55}Mn^{+}$	94.90043	6	
$^{40}Ar^{54}FeH^{+}$	94.90982	3	
^{107}Ag	**106.9051**		> 100
$^{91}Zr^{16}O^{+}$	106.9006	70	>10 without Zr
$^{90}Zr^{16}OH^{+}$	106.9074	12	
$^{89}Y^{18}O^{+}$	106.9050	1	
$^{181}Ta^{33}S^{+2}$	106.9597	1	
^{109}Ag	**108.9048**		> 10
$^{90}Zr^{19}F^{+}$	108.9031	8	>1 without Zr
$^{92}Zr^{16}OH^{+}$	108.9078	5	

Table 2. (continuation).

Isotope, molecular ion	Mass (m/q)	Maximal «concentration», ppm	Detection limit in dry sediment at $R_{0.5}$= 9000, ppm*
^{110}Cd	**109.9030**		> 700
$^{94}Zr^{16}O^{+}$	109.9012	590	>1 without Zr
$^{40}Ca_2{}^{14}N^{16}O^{+}$	109.9232	14	and Mo <10 ppm
$^{91}Zr^{19}F^{+}$	109.9041	9	
$^{94}Mo^{16}O^{+}$	109.9000	4	
^{111}Cd	**110.9042**		> 50
$^{94}Zr^{16}OH^{+}$	110.9091	23	>10 without Zr
$^{92}Zr^{19}F^{+}$	110.9034	14	
$^{95}Mo^{16}O^{+}$	110.9008	7	
$^{40}Ar_2{}^{31}P^{+}$	110.8985	6	
^{112}Cd	111.9028		> 80
$^{96}Zr^{16}O^{+}$	111.9032	50	>10 without Zr
$^{40}Ca_2{}^{32}S^{+}$	111.8972	6	
$^{40}Ca_2{}^{16}O_2{}^{+}$	111.9150	4	
^{202}Hg	**201.9706**		> 0.01
$^{40}ArH^{161}Dy^{+}$	201.8972	2	
$^{40}Ca^{162}Dy^{+}$	201.8894	1	
^{203}Tl	**202.9723**		> 0.1
$^{40}ArH^{162}Dy^{+}$	202.8970	0.3	
$^{40}Ca^{163}Dy^{+}$	202.8913	0.1	
^{205}Tl	204.9744		> 80
$^{181}Ta^{12}C_2{}^{+}$	204.9480	120	
^{208}Pb	207.9766		> 5
$^{181}Ta^{27}Al^{+}$	207.9296	12	

* - Detection limit is given also for more pure matrix without impurities creating major interferences.

Addition of Ag in HAP-implants is often used as antibacterial component that promotes more safe and rapid recovery after surgery. Comparison of isotopes ^{107}Ag and ^{109}Ag show intense interference $^{91}Zr^{16}O^{+}$ overlapping ^{107}Ag isotope in the presence of Zr impurities (Fig. 5 and Table 2). Correct analysis should be done under control of Zr-content. Calculated spectrum for ^{107}Ag correctly reproduces double charged ion $^{181}Ta^{33}S^{+2}$. Such resolved molecular ions may serve as additional mass-mark point in the case of temperature deviation of a spectrum.

Special group are formed rare earth elements. The most intense molecular ions are formed from REE and isotopes of gases (H, O, N) and also group around the isotope measured. Fortunately, such combinations, even at very high gases content, are less intensive than measured isotope. Considering rather stable proportion between REE (Fig. 4), every time more intense interference overlap more intensive REE isotope peak so in most cases interferences do not damage spectra. As a rule this may be validated by close values obtained for different isotopes of the same element (Table 1). But there is an exception for ^{155}Gd and ^{157}Gd where the first isotope is overlapped by strong molecular ion $^{139}La^{16}O^{+}$ [9] (Fig.6).

Characteristic feature of mass spectra of REE is the molecular peaks location in the narrow range from the left side of the isotope beginning from ^{157}Gd and further till the ^{238}U this shift grows, Fig.6. This effect is a result of mass defect and binding energy of nuclei and analysis of mass spectra deserves of separate article from this point of view.

Isotopes of ^{182}W and ^{183}W are overlapped by intense ions $^{181}TaH^{+}$, $^{181}TaH_2{}^{+}$ and do not meet requirements on detection limit, however isotopes ^{184}W, ^{186}W may be used with sensitivity > 10 ppm. Isotopes ^{187}Re, ^{191}Ir allow determination with detection limit > 1ppm. Unfortunately in this matrix no one Pt-isotope can not be measured with Ta-secondary cathode because of strong interferences of types TaX^{+} (X – O, N, C) and another cathode metal should be used (for instance – Al). Determination of Au with Ta-cathode in the matrix with high content of oxygen also can not be performed because the only gold isotope ^{197}Au overlapped by intense $^{181}Ta^{16}O^{+}$ molecular ion. Another heavier than Ta isotopes (^{202}Hg, ^{208}Pb, ^{209}Bi, ^{238}U) may be successfully used for analysis on the high resolution double focusing spectrometers with detection limit > 1 ppm.

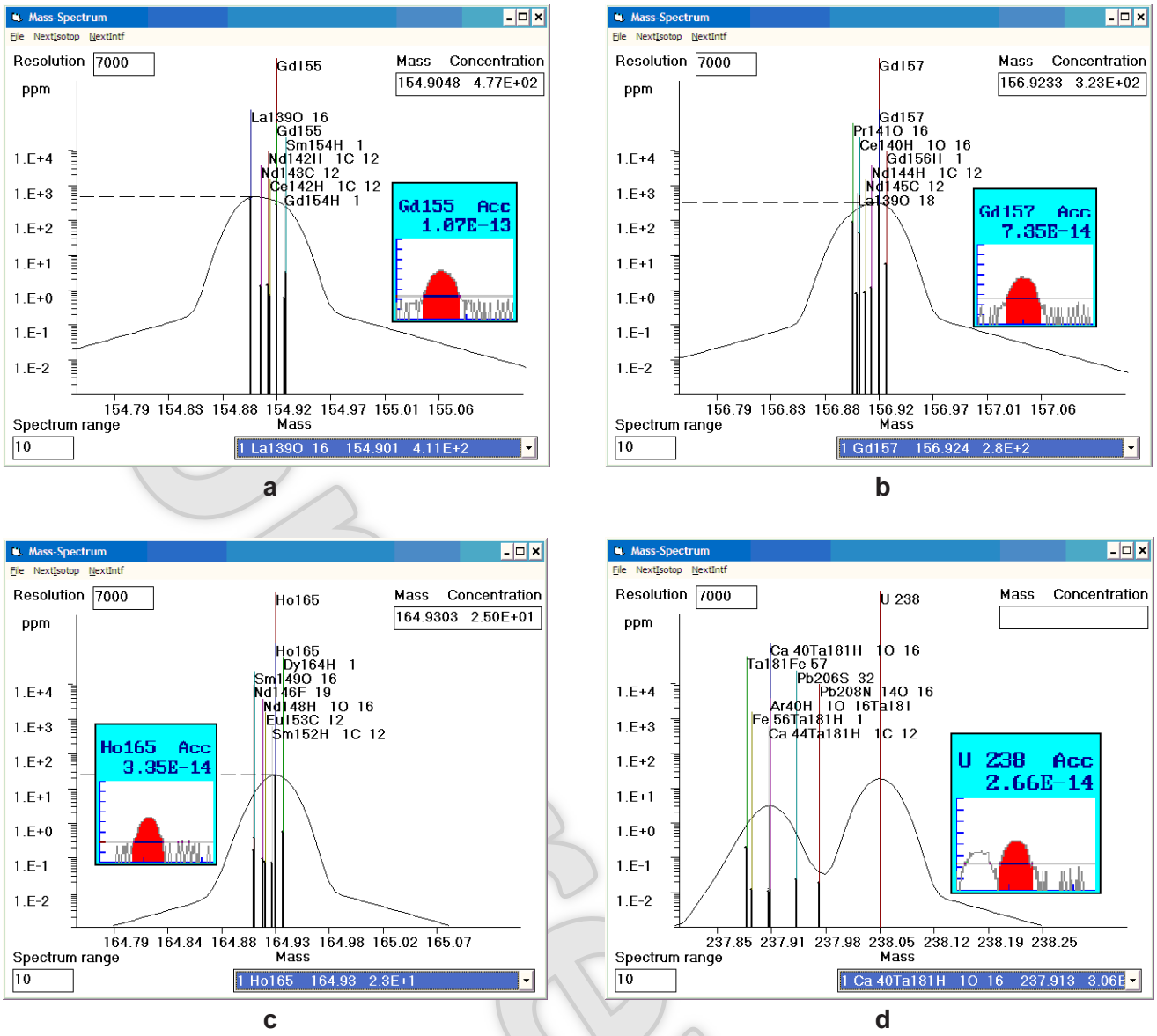

Fig. 6. Measured and calculated mass-spectra for several isotopes of REE and ^{238}U.

Conclusions

GDMS technique was developed for analysis of calcium carbonate naturally doped with REEs and other impurities that may be used as precursor for hydroxyapatite synthesis alloyed by REEs and Ag. An improved design of the cell with Ta-secondary cathode was suggested enhancing the matrix to tantalum ion current ratio and sensitivity of the analysis in ca. 1.5 orders of magnitude.

Although GD plasma is nonequilibrium object with “hot” electrons and “cold” heavy particles it have been shown that electrons obey Maxwell distribution in different plasma zones. Enhancing of ionization potential of components requires higher temperatures and ionization occurs in different zones. Electron temperature measured from Boltzmann plot increases in a series MeO^+, Me^+, Ar^{+1}– Ar^{+3}, Ar^{+4} – Ar^{+6} and is 0.75, 1.5, 4.5 and 7 eV respectively.

Interferences were calculated and simulation of mass-spectra were performed by the new version of the computer program allowing more precise calculation polyatomic ions on the basis refined effective equilibrium constants measured for matrix discussed. Sensitivity of the analysis was measured and calculated for more than 100 isotopes of the periodical system and the most important data concerning REEs and some biologically active elements are presented. Results show that detection limit depends on bulk composition of a sample and mass region, i.e. on molecular interferences and for the most elements 1–10 ppm sensitivity level is achieved in such a complex matrix. For more pure matrix ppb-level is quite possible that is good level for nonconducting samples.

References

1. King F.L., Harrison W.W. Collision-induced dissociation of polyatomic ions in glow discharge mass spectrometry. *Int. J. Mass Spectrom.* 1989, *89*(2–3), 171–185.

2. Fürstenau N., Hillenkamp F. Laser-induced cluster-ions from thin foils of metals and semiconductors. *Int. J. of Mass Spectrom.* 1981, *37*(2), 135–151.

3. Kurochkin V.D. Calculation of Intensities of Molecular Interferences in GD-MS: Application to Analysis of Aluminium Alloys. *Analytical Communications*. 1996, *33*, 381–384.

4. Thalagalage Shalika Harshani Perera, Yingchao Han, Xiaofei Lu at al. Rare Earth Doped Apatite Nanomaterials for Biological Application. *J. of Nanomaterials*, Hindawi Publishing Corporation, Volume 2015. http://dx.doi.org/10.1155/2015/705390.

5. Granados-Correa, F.; Vilchis-Granados, J.; Jiménez-Reyes, M.; at al. Adsorption Behaviour of La(III) and Eu(III) Ions from Aqueous Solutions by Hydroxyapatite: Kinetic, Isotherm, and Thermodynamic Studies. *Hindawi Publishing Corporation J. of Chemistry*, Volume 2013, Article ID 751696. http://dx.doi.org/10.1155/2013/751696

6. Yan-zhong Zhao, Min Yang , Hai-bin Zhang at al. Characterization of terbium-doped nano-hydroxyapatite and surface modification. *J. of Central South University*. 2016, *23*(7), 1548–1555.

7. Liliana Inconaru S., Motelica-Heino M., Predoi D. Study of europium doped hydroxyapatite by Fourier transform infrared spectroscopy and their antimicrobial properties. *J. of Spectroscopy*. 2013, Article AD 284285. http://dx.doi.org/10.1155/2013/284285

8. Milton D., Hutton J. C. Investigation into the suitability of using a secondary cathode to analyse glass using glow discharge mass spectrometry. *Spectrochim. Acta Part B*. 1993, *48*, 39–52.

9. Schelles W., De Gendt S., Van Grieken R. Optimization of secondary cathode thickness for direct current glow discharge mass spectrometric analysis of glass. *J. Anal. At. Spectrom*. 1996, *11*, 937–941.

10. Schelles W., De Gendt S., Maes K at al. The use of a secondary cathode to analyse solid non-conducting samples with direct current glow discharge mass spectrometry: potential and restrictions. *Fresenius' J. of Anal. Chemistry*. 1996, *355*(7–8), 858–860.

11. Schelles W., Van Grieken R. Quantitative analysis of zirconium oxide by direct current glow discharge mass spectrometry using a secondary cathode. *J. of Anal. Atomic. Spectrometry*. 1997, *12*, 49–52.

12. Tong S. L., Harrison W. W. Glow discharge mass spectrometric analysis of non-conducting materials. *Spectrochim. Acta*. 1993, *48B*, 1237–1245.

13. De Gendt S., Schelles W., Van Grieken, at al. Quantitative analysis of iron-rich and other oxide-based samples by means of glow discharge mass spectrometry. *J. Anal. At. Spectrom*. 1994, *10*, 681–687.

14. Winchester M. R., Duckworth D.C., Marcus R. K. Analysis of non-conducting samples. Glow Discharges Spectroscopies ; Ed. R.K. Marcus. - New York : Plenum, 1990. - P. 263–326.

15. Barshick C. M., Duckworth D. C., Smith D. H. Analysis of Solution Residues by Glow Discharge Mass Spectrometry. *J. Am. Soc. Mass Spectrom*. 1993, *4*, 47–53.

16. Shaw R. W., Barshick C. M., Ramsey J. M. at al. Metal Mesh Smear Sampling for Glow Discharge Analytical Spectroscopy: *Interim Technical Report* – [report] Chemical and Analytical Sciences Division Oak Ridge National Laboratory, 2000.

17. Kurochkin V.D., Kravchenko L.P. Analysis of impurities in high-purity aluminum oxide by glow discharge mass spectrometry. *Powder Metall. Met. Ceram*. 2006, *45*(9-10), 493-499.

18. Kurochkin V.D., Romanenko O.M., Skulsky M.O. Determination of REE and some toxic elements in mine waters of Donetsk region by GD-MS. *Methods objects Chem. Anal.* 2014, *9*(2) 59–64.

19. Kurochkin, V.D. Utvorennia ionnyh dymeriv z material katoda v krio-oholodzhuvaniy komirci v plasmi zhevriuchogo rozriadu. *Ukrainsky Chim. J*. 1999, *65*(3), 57–63.

20. Kurochkin, V.D. Osobennosti obrazovania argonsoderzhaschih molecularnyh ionov v krio-ohlazhdaemoi plasma tleiuschego razriada. *Ukrainsky Chim. J*. 2003, *69*(9), 26–34.

21. Vieth W., Huneke J. C. Studies on ion formation in a glow discharge mass spectrometry ion source. *Spectrochim. Acta Part B*, 1990, *45*(8), 941–949.

22. Gromet L.P., Dymek R.F., Haskin L.A. at al. The "North American shale composite": Its compilation, major and trace elements characteristics. *Geochim. et Cosmochim. Acta*, 1984, *48*, 2469–2482.

23. Kurochkin V.D. Izotopnyi analiz selena, zbagachenogo izotopom ^{74}Se na mas-spectrometre iz zhevriuchim rozriadom. *Ukrainsky Chim. J*. 2006, *72*(8), 103–107.